Energy-Tunable Sources of Entangled Photons: A Viable Concept for Solid-State-Based Quantum Relays

Article *in* Physical Review Letters · April 2015

DOI: 10.1103/PhysRevLett.114.150502 · Source: arXiv

CITATIONS
59

READS
125

4 authors:

Rinaldo Trotta
Sapienza University of Rome
148 PUBLICATIONS **2,338** CITATIONS
SEE PROFILE

Javier Martín-Sánchez
University of Oviedo
84 PUBLICATIONS **1,005** CITATIONS
SEE PROFILE

C. Ortix
Utrecht University
99 PUBLICATIONS **1,590** CITATIONS
SEE PROFILE

Armando Rastelli
Johannes Kepler University Linz
360 PUBLICATIONS **9,377** CITATIONS
SEE PROFILE

Energy-tunable sources of entangled photons: a realistic concept for solid-state quantum relays

Rinaldo Trotta,[1]* Javier Martín-Sánchez,[1] Carmine Ortix,[2] and Armando Rastelli[1]

[1]Institute of Semiconductor and Solid State Physics, Johannes Kepler University Linz, Altenbergerstr. 69, A-4040 Linz, Austria.

[2]Institute for Theoretical Solid State Physics, IFW Dresden, Helmholtzstr. 20, D-01069 Dresden, Germany.

We propose a new method of generating entangled photon pairs with wavelength on demand. The method uses a six-legged semiconductor-piezoelectric device capable of dynamically reshaping the electronic properties of self-assembled quantum dots via anisotropic strain-engineering. Theoretical models based on $\mathbf{k}\cdot\mathbf{p}$ theory in combination with finite element calculations are used to demonstrate that the energy of the polarization-entangled photons emitted by quantum dots can be tuned in a range larger than 100 meV without affecting the degree of entanglement of the quantum source. These results pave the way towards the deterministic implementation of QD entanglement resources in all electrically-controlled solid-state quantum relays.

Corresponding Author

Rinaldo Trotta

Institute of Semiconductor and Solid State Physics,

Johannes Kepler University Linz, Altenbergerstr. 69,

A-4040 Linz, Austria.

Tel.: +43 732 2468 9599

Fax: +43 732 2468 8650

e-mail: rinaldo.trotta@jku.at

Quantum communication deals with the transfer of quantum states from one place to another. One of its applications, quantum key distribution, promises secure data transmission by encoding "bits", e.g., in the polarization state of photons[1]. However, unavoidable transmission losses of the channel employed for the transmission of the quantum states limits the reachable distances to a few hundred of km. One elegant solution to this problem is the use of quantum repeaters[2], often referred to as the quantum analogous of classical amplifiers. Instead of regenerating the optical signal – as conventional amplifiers do – the idea behind quantum repeaters is to mitigate transmission losses by means of quantum relays, i.e., quantum devices capable to teleport or swap entanglement between distant nodes. A single quantum relay, sketched in Figure 1a, consists of two entanglement resources (ERs) emitting pairs of entangled photons. A Bell-state measurement (BSM) between photons emitted by the two remote ERs allows entanglement to be distributed over distant nodes. A partial BSM can be obtained by Hong-Ou-Mandel (HOM) type two-photon interference[3]. This quantum-mechanical phenomenon consisting in the coalescence of two single-photon states into a two-photon collective state has been employed in the first demonstration of entanglement swapping[4], and has been recently implemented using independent photon sources[5,6] including optically active semiconductor quantum dots (QDs)[7,8].

Often referred to as “artificial atoms”, QDs are semiconductor nanostructures capable of deterministic generation of high-quality single[9] and entangled[10] photons and, unlike other quantum emitters, can be easily integrated into well-established optoelectronic devices[11]. Therefore, semiconductor QDs are very attractive ERs. Figure 1b sketches the scheme usually employed for the generation of polarization-entangled

photon-pairs emitted during the radiative cascade of a confined biexciton (XX) to the exciton (X) to the crystal ground state[12]. With such a scheme in mind, one could dream to build-up a quantum relay using two identical QDs and use HOM interference[3] of the XX photons to entangle the X photons (see Figure 1b). In spite of the simplicity of the proposed scheme, the possibility of using QDs as a truly viable building block for quantum relays requires a number of extraordinary challenges to be overcome. The problems related to the need of Fourier-limited[13,14] , bright[15,16,17] and site-controlled[18] photon sources have been recently successfully addressed. There is another issue, however, which is still open: different from real atoms, each QD possesses its own size, shape, and composition[19] and, as a consequence, unique emission spectra. This hurdle has a dramatic impact on the proposed scheme for quantum relays (see Figure 1c). First, there are no identical QDs in reality. Considering that the inhomogenous broadening of QD emission is ~ tens of meV, the probability of finding two QDs for which photons emitted by XX (or X) have the same energy within typical radiative-limited emission linewidth (~μeV) is $< 10^{-4}$. If we restrict our discussion to Fourier-limited photons, this fact eventually prevents the possibility of performing BSM, because the colour difference between the photons prevents their interaction at the beam splitter[7,8]. The second hurdle arises from the anisotropic electron-hole exchange interaction[20], which generally leads to the appearance of a fine-structure splitting (FSS, s) between the two bright X states (see Fig. 1c). When the FSS is larger than the radiative-limited emission linewidth of the X transition, the capability of a QD to generate photon pairs featuring high degree of entanglement – high enough to violate Bell's inequalities without the use of inefficient temporal filtering techniques[11]– is severely hampered. Recent theoretical calculations[21]

show that only a very low portion of as-grown QDs are free of asymmetries (1 over 1000 for Stransky-Kranstanov QDs) and the numbers increase little if very sophisticated growth protocols are employed[18]. Therefore, the probability of finding two as-grown QDs suitable to swap entanglement is considerably small (10^{-9} or less), and it is practically zero in the case of protocols involving several sources. These hurdles have naturally led to the idea of post-growth tuning of the QD emission properties via the application of external perturbations, such as strain[22], electric[23] and magnetic[24] fields. It turned out, however, that even with the aid of external "tuning knobs" it is extremely difficult to implement the scheme of Figure 1b. Some of us have recently found a universal method to tune every single QD in the ensemble for the generation of high-quality entangled photons[25,26]. The method relies on the simultaneous application of independent external perturbations – in particular strain and electric field – to systematically suppress the FSS. Despite this result shows that the tedious search for QDs suitable as ERs can be avoided, the energy of the entangled photons emitted by remote QDs is generally different, and any attempt to modify the magnitude of strain and electric field so as to achieve colour matching restores the FSS and spoils entanglement.

In this letter, we propose a realistic concept for an energy-tunable source of polarization entangled photons, which can be exploited for the implementation of QD-based quantum relays. The key idea is to use anisotropic-strain engineering of the semiconductor matrix hosting the quantum emitters to reshape their electronic structure so that entanglement swapping becomes possible (see Figure 1e). By using theoretical models for the exciton Hamiltonian, we show how full control of in-plane stress allows the energy of the entangled photons emitted during the XX-X-0 radiative cascade to be

modified without affecting the degree of entanglement, i.e, without restoring the FSS. We then propose a realistic device (see Figure 1d) that can successfully address this task: It consists of a micro-machined single crystal $[Pb(Mg_{1/3}Nb_{2/3})O_3]_{0.72}$-$[PbTiO_3]_{0.28}$ (PMN-PT) piezoelectric actuator featuring six legs and capable of deforming in any direction a GaAs nanomembrane containing QDs. Finite element calculations (FEM) combined with **k·p** models are then used to demonstrate (i) that the application of three independent voltages on pairs of aligned legs allows stress anisotropies to be engineered on demand with magnitudes as large as 0.6 GPa and (ii) that the energy of the entangled photons emitted by QDs can be modified over a spectral range larger than 100 meV. Since the latter value is much larger than the inhomogeneous broadening of self-assembled QD ensemble, the hybrid semiconductor-piezoelectric device we propose in this work paves the way towards a deterministic implementation of QD entanglement resources for solid-state quantum relays.

We start out presenting the theory underlying the development of energy-tunable source of entangled photons. In standard self-assembled QDs, the coupling of electrons and heavy-holes results in four degenerate excitonic states denoted as dark (total angular momentum M=±2) and bright (M=±1) depending on whether they do couple to the photon field or not. Independent of the symmetry of the confining potential, the electron-hole exchange interaction causes a splitting between the dark and bright states. On the other hand, the symmetry of the confining potential is of fundamental importance for the fine structure of the bright doublet[20]. A structural symmetry lowering from C_{4v}/D_{2d} to C_{2V} yields to a coherent coupling of the two bright states and, as a result, to the appearance of the FSS. As the two non-degenerate bright excitons $|B_{\pm}\rangle = |1\rangle \pm |-1\rangle$ now belong to two

different irreducible representations ($\Gamma_{2,4}$) , a single external perturbation can act as an effective knob to tune the FSS, eventually restoring the level degeneracy. In real QDs, however, strain, piezoelectricity, and alloying further lower the structural symmetry to C_1. Besides a renormalization of the FSS, these effects introduce an additional mixing of the $|B_{\pm}\rangle$ states and cause the polarization direction of the exciton emission to depart from the [110] and [1-10] crystal directions generically expected for the case of C_{2v} QDs[27]. To show this, we consider an effective two-level Hamiltonian in the $|B_{\pm}\rangle$ basis:

$$H = E_0\tau_0 + \eta\tau_z + k\tau_x, \qquad (1)$$

where the τ 's are the usual Pauli matrices with $\tau_0 = I_2$, i.e., the identity matrix. In Equation 1, E_0 indicates the energy of an exciton confined in a highly symmetric C_{4v}/D_{2d} QD, whereas η and k account for the lowering of the structural symmetry to C_1 and lead to two non-degenerate transitions at $E = E_0 \pm \sqrt{\eta^2 + k^2}$. The polarization of the exciton emission can now be inferred from the eigenvectors of the Hamiltonian, $|\psi_{\pm}\rangle = k|B_+\rangle + \left(\eta \pm \sqrt{\eta^2 + k^2}\right)|B_-\rangle$, implying a polarization angle $\tan\theta_{\pm} = \left(\eta \pm \sqrt{\eta^2 + k^2}\right)/k$ with respect to the [110] crystal direction. Because the two bright excitons now belong to the same irreducible representation Γ_1 , the Wigner-von Neumann non-crossing rule[28] is in full force and single external fields are in general not sufficient to suppress the FSS[27,29]. Rather, the two bright exciton states will repel each other leading to an avoided level crossing and to a lower bound for the FSS[29]. As shown in previous works[25,30], this problem can be circumvented in any QD by the simultaneous application of two external fields. From a theoretical point of view, this is possible because the two different external fields are always capable of satisfying – effectively – the constraints of exciton level

degeneracy, that is $\left\langle B_+ \left| H_{eff} \right| B_- \right\rangle \equiv 0$ and $\left\langle B_+ \left| H_{eff} \right| B_+ \right\rangle \equiv \left\langle B_- \left| H_{eff} \right| B_- \right\rangle$, where H_{eff} is the exciton Hamiltonian in the presence of the two external fields. At this point, it is quite clear that three independent external fields are required to build-up an energy tunable source of entangled photons: two fields are taken up to fulfill the condition of level degeneracy, while the third field is needed to control independently the X energy. To achieve such a goal, one could combine strain and electric fields[25] with a third control field, such as an external magnetic[24] or optical field[31]. This idea, however, is not convenient in the perspective of real applications, since it requires the use of bulky experimental set-ups. We instead show that in-plane stress fields naturally offer three independent control knobs to successfully address this task, as they are characterized by three components of the stress tensor, $\sigma_{xx}, \sigma_{yy}, \sigma_{xy}$ or equivalently, by two principal (perpendicular) stresses S_1, S_2 and an angle ϕ with respect to the [110] crystal direction (see Figure 2a). The strain Hamiltonian can be written as

$$\delta H_s = \bar{\alpha} \cdot \bar{p}\,\tau_0 + \alpha \cdot \Delta p \cdot \cos(2\phi)\tau_z + \gamma \cdot \Delta p \cdot \sin(2\phi)\tau_x \qquad (2)$$

where $\bar{\alpha}, \alpha$ are effective parameters related to the elastic compliance constants renormalized by the valence band deformation potentials and we have introduced $\bar{p} = S_1 + S_2$ (hydrostatic part) and $\Delta p = S_1 - S_2$ (stress anisotropy). Three parameters are therefore relevant to the problem: $\bar{p}$, Δp, and ϕ. Their effect on the exciton Hamiltonian is twofold. First, by properly setting ϕ such that the strain principal direction is parallel to the polarization direction of the exciton emission θ_+, the level degeneracy can be restored by simply adjusting the magnitude of Δp. To see that more clearly, it is sufficient to impose the condition of level degeneracy – which leads us to

$\eta = -\alpha \cdot \Delta p \cdot \cos(2\phi)$ and $k = -\gamma \cdot \Delta p \cdot \sin(2\phi)$ – and to remember that the principal directions of the stress tensor ϕ are rotated with respect to the principal directions of strain ϕ_ε via the following formula: $\tan 2\phi = -\frac{S_{44}}{2(S_{11}-S_{12})}\tan 2\phi_\varepsilon$, where S_{ij} are the elastic compliance constants. The FSS can now be suppressed once the stress is applied at an angle $\phi = \phi^*$ such that ϕ_ε takes the following value $\tan 2\phi_\varepsilon{}^* = \frac{2(S_{11}-S_{12})}{S_{44}}\frac{\alpha}{\gamma}\tan 2\theta_+$, yielding $\phi_\varepsilon{}^* \approx \theta_+$ when the numerical prefactor is on the order of one. In order to give a realistic estimation of the difference between $\phi_\varepsilon{}^*$ and θ_+, we account for strain-induced effects using the Dresselhaus-Kip-Kittel Hamiltonian [32] which allows us to calculate the effective parameters α and γ considering the values of the elastic compliance constants and the valence band deformation potentials in bulk GaAs and InAs. Apart from a slight larger deviation for the case of GaAs QDs, Figure 2a clearly shows that the excitonic degeneracy can be restored in any QD when the stress is applied at an angle ϕ^* such that $\phi_\varepsilon{}^* \approx \theta_+$. This accounts for the intuitive idea that the FSS can be suppressed once the perturbation (strain) is precisely aligned along the polarization direction of the exciton emission so that it can compensate completely – at certain Δp – for the asymmetries of the QD confining potential. This can be seen even more clearly in Figure 2b, where a parametric plot of the FSS is reported against the energy of X for different values of $\phi_\varepsilon{}^*$ in a InAs QD featuring θ_+=-16.2°. It is clear that s=0 is achieved only for a specific value of ϕ^* such that $\phi_\varepsilon{}^* \approx \theta_+$. For all the other angles, a lower bound of the FSS is observed. We highlight once more that two control parameters (ϕ and Δp) are required to suppress the FSS, in complete agreement with previous experimental results[25]. The

second important strain-related effect comes about the hydrostatic contribution $\bar{p}$ (third control parameter), which influences the X energy without affecting the structural symmetry of the QD (possible effects on the FSS due to band-offset changes and consequent electro-overlap changes[33,34], as well as shear-stress-induced piezoelectricity are not considered here). The black lines of Figure 2b show that it is indeed possible to find values of S_1 and S_2 such that ϕ^* and Δp^* are constant at the values required for s=0, while $\bar{p}$, proportional to the X energy, varies. These theoretical calculations do not only indicate that the energy of the entangled photons can be tuned at will without affecting the FSS, but they also suggest a three step procedure to achieve this result experimentally: (step 1) align the major stress axis to ϕ^* such that the major strain axis is aligned along the polarization direction of the exciton emission, i.e., $\phi_\varepsilon^* \approx \theta_+$; (step 2) change the magnitude of $\Delta p = S_1 - S_2$ keeping fixed ϕ at ϕ^* until the condition of s=0 is reached. This occurs for $\phi = \phi^*$ and $\Delta p = \Delta p^*$. In the Figure 2b, step 2 is performed varying S_1 at $S_2 = 0$; (Step 3) modify $\bar{p} = S_1 + S_2$ at fixed $\phi = \phi^*$ and $\Delta p = \Delta p^*$ so as to change at will the X energy. In the Figure 2b this is achieved by sweeping again S_1 at different values of S_2 (see the different black lines in the Figure 2b). Since the QD parameters are fixed, the condition of s=0 is found exactly at the same values of $\phi = \phi^*$ and $\Delta p = \Delta p^*$ but for a different combination of S_1 and S_2 and, as a consequence, for different X energies. The range of tunability achievable in real experiments depends on the QD structural details and on the magnitude of S_1 and S_2 reachable in real experiments. Using QD parameters estimated in our previous work[25], assuming maximum values of S_1 and S_2 ~ 0.6 GPa (see the following), and taking into account the

experimental value[34] of the shift of the X energy with hydrostatic stress (so as to include strain-related effect on the conduction band), we predict that at s=0 the X energy can be controlled in a range as large as 100 meV (see Figure 2b). It is important to highlight that the three-step procedure discussed above can be tested experimentally. All the relevant quantities of the problem can be measured by looking at the QD optical spectra– which allows for determination of θ and s – and at the emission stemming from the recombination of the two strain-split free excitons (in general involving mixtures of light- and heavy holes) in the bulk semiconducting matrix. As the deformation potential for (Al)GaAs are known, S_1, S_2, and ϕ can be easily inferred using well-tested **k·p** models[35]. At this point, it is quite clear that the success of our proposal is strictly connected to the capability of achieving independent control of S_1, S_2, and ϕ. The way how to achieve this task experimentally without spoiling optical access and still enabling electrical control is not obvious and is demonstrated in the following.

The device concept we propose here as energy-tunable source of entangled photons consists of a micro-machined single crystal PMN-PT piezoelectric actuator featuring six legs aligned at a 60° angle with each other[36] and hosting a ~300 nm thick Al(GaAs) nanomembrane containing single In(Ga)As QDs, see sketch of Figure 1d. The central area where the nanomembrane is suspended is the active region, where anisotropic stress-fields exerted by the device engineer the QD electronic properties. The geometry of the legs has been inspired by the following key idea: full control of the in-plane stress tensor can be achieved via the simultaneous application of three independent uniaxial stresses in the plane perpendicular to the growth direction of the membrane under study ((001) or (111) of the (Al)GaAs crystal). In our device, quasi-uniaxial

stresses are achieved by applying three independent voltages (V_1, V_2, V_3) on contacts defined at the bottom of the legs, while the top is electrically grounded to avoid any electric perturbation to the QD structure (see Figure 1d). The voltages induce electric fields in the piezoelectric legs that lead to an in-plane contraction/extension of the material and, in turn, to a deformation of the nanomembrane in the same direction. The magnitude and compressive/tensile character of the in-plane stress on the piezo- legs, i.e., on the nanomembrane, can be controlled by selecting the appropriate voltage magnitude and sign, respectively. The same voltage is applied to opposite legs to limit displacements of the central structure. It is worth noticing that in the configuration shown in the Figure 1d – where the central gap between the piezo-legs (300 μm) is shorter than the piezo-legs length (1500 μm) – one expects strongly enhanced strain values on the central part of the membrane due to a geometrical "focusing" effect, similar to Ref.[37].

We now demonstrate that the proposed device allows for full control over the components of the in-plane stress tensor (σ_{xx}, σ_{yy}, σ_{xy}, or strain, linked to stress by the compliance) or, equivalently, of S_1, S_2, and ϕ. To do so, finite element simulations were performed (using COMSOL multiphysics software) on the proposed device with realistic parameters for elastic/piezoelectric properties for a 200 μm-thick PMN-PT and a 300 nm-thick GaAs membrane. Considering linearity in elasticity theory, the voltage sets required to obtain a given stress configuration can be predicted by using the expression $(V_1, V_2, V_3) = \underline{\underline{R}}^{-1}(\sigma_{xx}, \sigma_{yy}, \sigma_{xy})$, where $\underline{\underline{R}}$ is a 3×3 transfer matrix which can be obtained using a small set of FEM simulations. Our FEM analysis suggests that by using reasonable voltages on the piezo-legs we can achieve full control of in-plane stress: Figure 3a shows FEM simulations for $V_1=V_3=0$ and $V_2=200$ V (top panel of Figure 3a)

and V_2=V_3=0 and V_1=200 V (bottom panel of Figure 3a). These sets of voltages allows the uniaxial major stress (S_1) axis to be rotated by 120° with respect to the [100] direction of the GaAs matrix (see insets of Figure 3a), with magnitudes as large as 0.6 GPa for a moderated electric field value of E~15 kV/cm. This predictive approach (FEM) can now be combined with the $\mathbf{k}\cdot\mathbf{p}$ model presented in the previous section to obtain a realistic estimation of the tunability of X energies at s=0. The FEM data were taken from the central part of the nanomembrane by averaging on a cylindrical volume of 10x10x0.3 μm^3. As detailed in the three-step procedure outlined above, we are interested in investigating the capability of the proposed device to tune the X energy (proportional to $\bar{p} = S_1 + S_2$) at fixed stress anisotropy, i.e., at fixed Δp and ϕ. The results are displayed in Figure 3b, where the X energy is plotted in cylindrical coordinates against the stress anisotropy (S_1-S_2) and major stress angle (ϕ). Considering that the Δp values required to cancel the FSS in standard QDs[25] are in the MPa range (see the Figure 2b), Figure 3b not only demonstrates full control of ϕ and Δp, but also a X energy shift up to the impressive value of 100 meV for fixed $\phi = \phi^*$ and $\Delta p = \Delta p^*$ (see the central area of Figure 3b), the limitation being the largest voltages that can be applied to the device before electrical breakdown or mechanical fracture of the membrane bonding layer occurs. Because of the strain-focusing effect discussed above, the latter issue is expected to limit the tuning range rather than the failure of the piezoelectric material. We have therefore theoretically demonstrated that the proposed six-legged device can act as an energy-tunable source of entangled photons. Its experimental realization is perfectly feasible considering nowadays processing technologies. The six-legged piezoelectric actuator can be conveniently fabricated by femtosecond laser cut of single crystal

substrates, as demonstrated by preliminary results (not shown). Conventional processing using well-established epitaxial lift-off techniques can be exploited to fabricate the (Al)GaAs nanomembranes, and their integration onto the piezoelectric actuator can be done following several approaches such as gold-thermocompression bonding[38], or eutectic bonding with SnAu commonly used for soldering optoelectronic devices. The latter route is particularly promising, as it requires low process pressures – with reduced risks of mechanical damages during the nanomembrane transfer – and it promises voidless soldering due to the fact that the SnAu is liquid at the process temperature.

The chosen device design offers additional interesting possibilities in the perspective of real applications. Firstly, the built-in metal layer used to integrate the nanomembrane onto the piezoelectric actuator can act as a mirror of a planar cavitiy. Beside the simple metal-semiconductor-dielectric planar cavity we have successfully implemented in previous works[38], more advanced approaches can be pursued for boosting the flux of QD photons (particularly important in quantum relay protocols). Among the others[39], photonic membranes featuring deterministic GaAs-microlenses[40] are particularly promising, since they can be easily integrated in our device design and would allow achieving extraction efficiency as high as 60%[39,41]. On the other hand, the metal layer can be used as additional contact for controlling the electric field across QDs embedded in diode-like-structures[23]. The electric field can then be used for injecting carriers electrically – as in standard light emitting diode[11] – or to tune the QD energy levels in synergy with strain to achieve independent control of X and XX energies[42]. The latter feature could pave the way for the realization of a complete quantum repeater[2], since it

would allow, e.g., for the storing of the X photons in warm atomic vapors while the XX photons are taken up for partial BSM.

Figure 1. Six legged piezoelectric actuator for solid state quantum relay. **(a)**. Sketch of a quantum relay. Yellow lines represent entanglement. Photodetectors are in black. BSM indicates Bell state measurement between photons emitted by separate sources while ER indicates entanglement resource. **(b)** Implementation with two identical QDs (unrealistic situation) using the radiative decay of the biexciton (XX) to the exciton (X) to the crystal ground state (0) for the production of polarization entangled photon pairs. σ^+ (σ^-) indicates right (left) circularly polarized photons. A partial Bell state measurement is performed via two-photon interference at a beam splitter (blu bar) followed by polarization resolved detection (polarizing beam splitters and detectors). **(c)** Realistic situation: The excitonic fine structure spitting (FSS) splits and mixes the two bright exciton states, thus spoiling the time-average entanglement between the emitted photons. H (V) indicates horizontally (vertically) polarized photons. The colour difference between photons from the remote QDs prevents their interaction at the beam splitter and, therefore, partial BSM. **(d)**. Schematic sketch of the six-legged micro-machined device proposed in this work. The top and bottom views are depicted on the left and right panel, respectively. Three independent voltages (V_1, V_2 and V_3) are applied on pairs of piezo-legs so as to engineer the strain status of an overlying semiconductor nano-membrane containing QDs and suspended in the central part. **(e)**. Same as in (b) for two QDs embedded in the hybrid device shown in (d), which allows fine-tuning the energy of the entangled photons emitted by the two remote QDs so as the match the conditions required for entanglement swapping.

Figure 2. Energy-tunable sources of polarization entangled photons. **(a)**. Mismatch between the polarization direction of the exciton emission (θ_+) and the direction of the major strain axis (ϕ_ε) in the condition when stress is fine-tuned for the suppression of the FSS, i.e, $\phi_\varepsilon = \phi_\varepsilon^*$. The blue (red) line indicates the result for InAs (GaAs) QDs. The inset shows a sketch of a single semiconductor QD featuring C_1 structural symmetry. The polarization direction of the exciton emission is also indicated, θ_+. The external anisotropic in-plane stress acting onto the QD is decomposed into the major (S_1) and minor (S_2) stresses applied at an angle ϕ with respect to the [110] crystal direction. **(b)**. Parametric plot of the FSS against the X energy (proportional to S_1+S_2) for a InAs QD with θ_+=-16.2˚ and subjected to different anisotropic in-plane stresses. The exciton energy is modified by varying S_1 at different values of the parameter S_2. The colored lines correspond to stresses applied along ϕ=-23˚ (purple line), ϕ=0˚ (red line), and ϕ=-12˚ (blue line) and with S_2=0. The black lines correspond to the condition of $\phi_\varepsilon = \phi_\varepsilon^*$=-18.5˚ and for three different values of S_2 =0, 0.3 and 600 MPa, from left to right respectively. The values of the ϕ_ε^* Δp^* and $\bar{p}$ at which s=0 are also indicated.

Figure 3. Performances of the six legged device. (a). Finite element simulations (FEM) in false color scale of the in-plane major stress for two sets of voltages applied to the six-legged device: V_2=200 V , V_1=V_3=0 V (top panel) and V_3=200 V and V_1=V_2=0 V (bottom panel). The inset of each panel shows a zoom of the central region containing the QDs and the angle formed by the major stress with respect to the [110] crystal direction of the membrane. **(b)**. X energy (in false color scale) as a function of the stress anisotropy

and major stress angle for voltages (V_1,V_2,V_3) in the range ±200 V. A cylindrical coordinate system has been used.

ACKNOWLEDGMENT

We thank J. S. Wildmann, T. Lettner, for fruitful discussions and I. Daruka for help during the first stage of the work. The work was supported financially by the European Union Seventh Framework Programme 209 (FP7/2007-2013) under Grant Agreement No. 601126 210 (HANAS), and the AWS Austria Wirtschaftsservice, PRIZE Programme, under Grant No. P1308457.

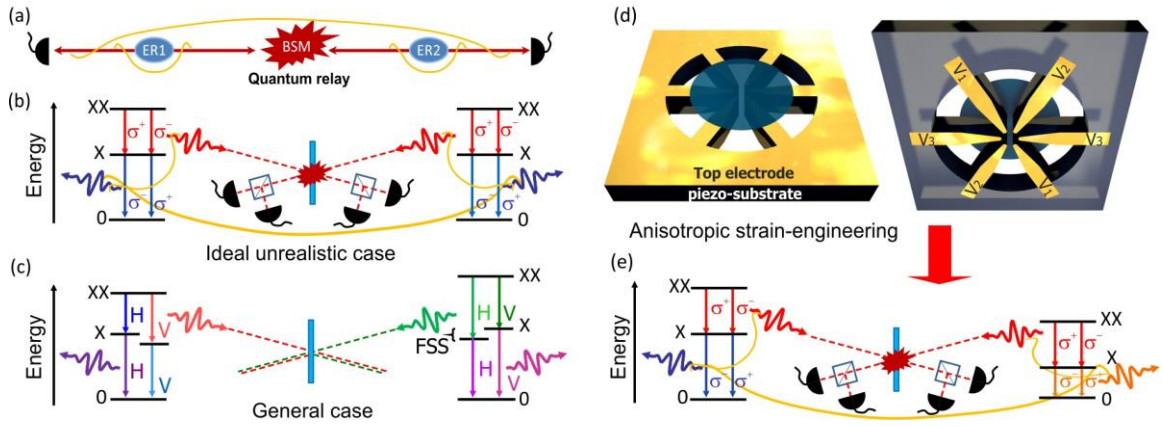

Figure 1 of 3

by R. Trotta et al.

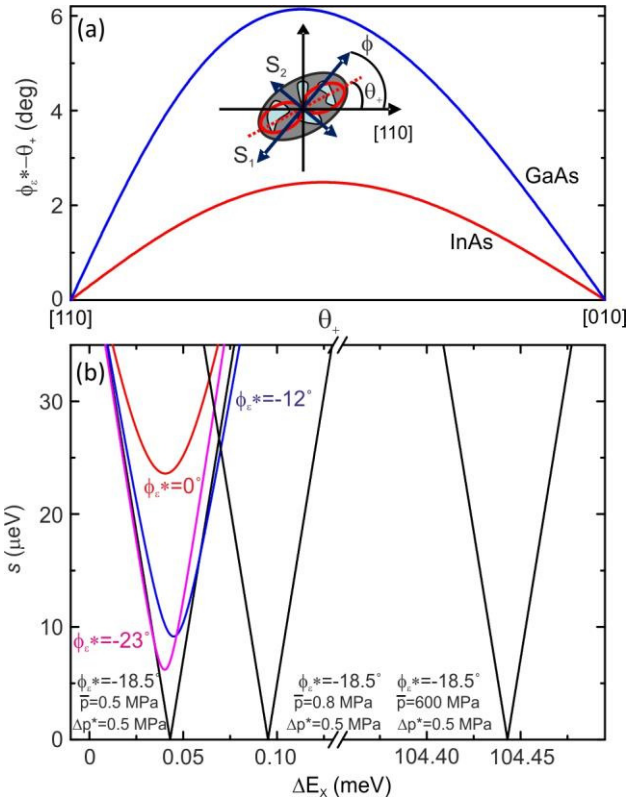

Figure 2 of 3

by R. Trotta et al.

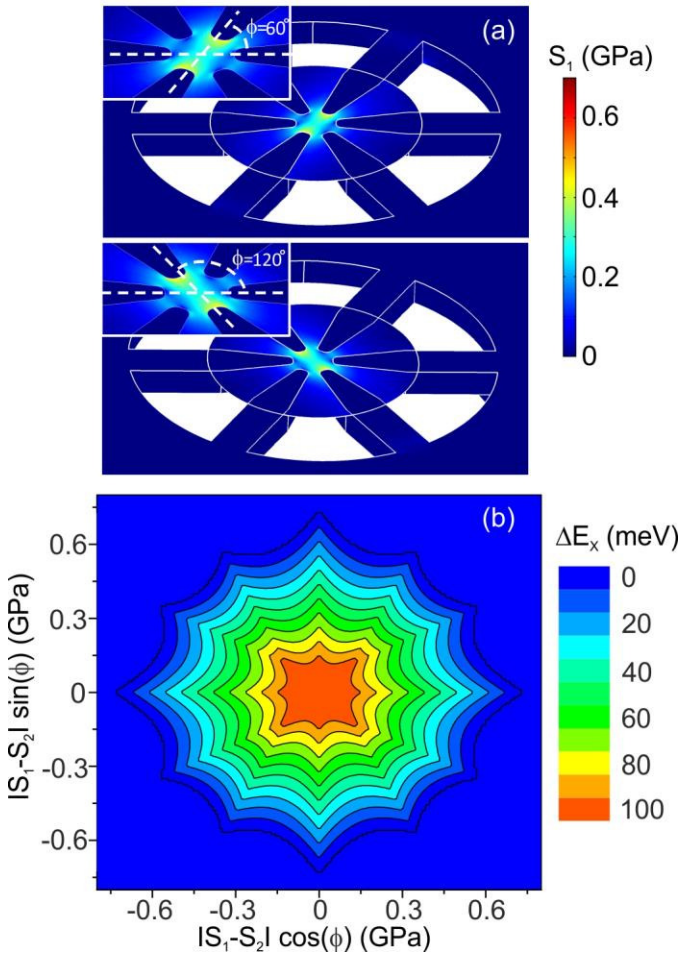

Figure 3 of 3

by R. Trotta et al.

[1] N. Gisin, G. Ribordy, W. Tittel, and H. Zbinden, Rev. Mod. Phys. **74**, 145 (2002)

[2] L.-M. Duan, M. D. Lukin, J. I. Cirac, and P. Zoller, Nature **414**, 413 (2001)

[3] C. K. Hong, Z.Y. Ou, and L. Mandel, Phys. Rev. Lett. **59**, 2044 (1987)

[4] J.-W. Pan, D. Bouwmeester, A. Zeilinger, Phys. Rev. Lett. **80**, 3891 (1998)

[5] J. Beugnon, M. P. A. Jones, J. Dingjan, B. Darquié, G. Messin, A. Browaeys and P. Grangier, Nature **440**, 779 (2006)

[6] P. Maunz, D. L. Moehring, S. Olmschenk, K. C. Younge, D. N. Matsukevich and C. Monroe, Nat. Phys. **3**, 538 (2007)

[7] R. B. Patel, A. J. Bennett, I. Farrer, C. A. Nicoll, D. A. Ritchie and A.J. Shields, Nature Photon. **4,** 632 (2010)

[8] E. B. Flagg, A. Muller, Sergey V. Polyakov, A. Ling, A. Migdall, and G. S. Solomon, Phys. Rev. Lett. **104,** 137401 (2010)

[9] P. Michler, A. Kiraz, C. Becher, W. V. Schoenfeld, P. M. Petroff, Lidong Zhang, E. Hu, A. Imamoglu, Science **290**, 2282 (2000)

[10] N. Akopian, N. H. Lindner, E. Poem, Y. Berlatzky, J. Avron, D. Gershoni, B. D. Gerardot, and P. M. Petroff, Phys. Rev. Lett. **96**, 130501(2006)

[11] C. L. Salter, R. M. Stevenson, I. Farrer, C. A. Nicoll, D. A. Ritchie and A. J. Shields, Nature **465**, 594 (2010)

[12] O. Benson, C. Santori, M. Pelton, and Y. Yamamoto, Phys. Rev. Lett. **84**, 2513 (2000)

[13] Y.-M. He, Y. He, Y.-J. Wei, D. Wu, M. Atatüre, C. Schneider, S. Höfling, M. Kamp, C.-Y. Lu, and J.–W. Pan, Nature Nanot. **8**, 213 (2013)

[14] M. Müller, S. Bounouar, K. D. Jöns, M. Glässl and P. Michler, Nature Phot. **8**, 224 (2014)

[15] A. Dousse, J. Suffczyński, A. Beveratos, O. Krebs, A. Lemaître, I. Sagnes, J. Bloch, P. and P. Senellart, Nature **466**, 217 (2010).

[16] M. A. M. Versteegh, M. E. Reimer, K. D. Jöns, D. Dalacu, P. J. Poole, A. Gulinatti, A. Giudice, and V. Zwiller, Nature Comm. **5**, 5298 (2014)

[17] T. Huber, A. Predojević, M. Khoshnegar, D. Delacu, P. J. Poole, H. Majedi and G. Weihs, Nano Lett., **14**, 7107 (2014)

[18] G. Juska, V. Dimastrodonato, L. O. Mereni, A. Gocalinska, and E. Pelucchi, Nature Phot. **7**, 527 (2013)

[19] A. Rastelli, M. Stoffel, A. Malachias, T. Merdzhanova, G. Katsaros, K. Kern, T. H. Metzger, O. G. Schmidt, Nano Lett. **8**, 1404 (2008)

[20] M. Bayer, G. Ortner, O. Stern, A. Kuther, A. A. Gorbunov, A. Forchel, P. Hawrylak, S. Fafard, K. Hinzer, T. L. Reinecke, S. N. Walck, J. P. Reithmaier, F. Klopf, and F. Schäfer, Phys. Rev. B **65**, 195315 (2002)

[21] M. Gong, B. Hofer, E. Zallo, R. Trotta, J.-W. Luo, O. G. Schmidt, and C. Zhang, Physical Review B **89**, 205312 (2014)

[22] S. Seidl, M. Kroner, A. Högele, K. Karrai, R. J. Warburton, A. Badolato and P. M. Petroff, Appl. Phys. Lett. **88**, 203113 (2006)

[23] A. J. Bennett, M. A. Pooley, R. M. Stevenson, M. B. Ward, R. B. Patel, A. Boyer de la Giroday, N. Sköld, I. Farrer, C. A. Nicoll, D. A. Ritchie and A. J. Shields, Nature Phys. **6**, 947 (2010)

[24] R. M. Stevenson, R. J. Young, P. Atkinson, K. Cooper, D. A. Ritchie and A. J. Shields, Nature (London) **439**, 179 (2006)

[25] R. Trotta, E. Zallo, C. Ortix, P. Atkinson, J. D. Plumhof, J. van den Brink, A. Rastelli, and O. G. Schmidt, Phys. Rev. Lett. **109**, 147401 (2012)

[26] R. Trotta, J. S. Wildmann, E. Zallo, O. G. Schmidt, and A. Rastelli, Nano Lett. **14** 3439 (2014)

[27] M. Gong, W. Zhang, G. –C. Guo, and L. He., Phys. Rev. Lett. **106**, 227401 (2011)

[28] J. von Neumann, and E. P. Wigner, Z. Physik **30**, 467 (1929)

[29] R. Singh, and G. Bester, Phys. Rev. Lett. **104**, 196803 (2010)

[30] J. Wang, M. Gong, G. Guo, and L. He, Appl. Phys. Lett. **101**, 063114 (2012)

[31] A. Muller, W. Fang, J. Lawall, and G. S. Solomon, Phys. Rev. Lett. **103**, 217402 (2009).

[32] L. C. L. Y. Voon and M. Willatzen, The k·p method: Electronic Properties of Semiconductors (Springer, Berlin, 2009)

[33] F. Ding, R. Singh, J. D. Plumhof, T. Zander, V. Křápek, Y. H. Chen, M. Benyoucef, V. Zwiller, K. Dörr, G. Bester, A. Rastelli, and O. G. Schmidt, Phys. Rev. Lett. **104,** 067405 (2010)

[34] X. F. Wu, H. Wei, X. M. Dou, K. Ding, Y. Yu, H. Q. Ni, Z. C. Niu, Y. Ji, S. S. Li, D. S. Jiang, G.-C. Guo, L. X. He and B. Q. Sun., Eur. Phys. Lett. **107,** 27008 (2014).

[35] F. H. Pollak, and M. Cardona, Phys. Rev. **172**, 816 (1968)

[36] A. Rastelli, I. Daruka, and R. Trotta (patent pending)

[37] M. J. Süess, R. Geiger, R. A. Minamisawa, G. Schiefler, J. Frigerio, D. Chrastina, G. Isella, R. Spolenak, J. Faist and H. Sigg, Nature Phot. **7**, 466 (2013)

[38] R. Trotta, P. Atkinson, J. D. Plumhof, E. Zallo, R. O. Rezaev, S. Kumar, S. Baunack, J. R. Schröter, A. Rastelli, and O. G. Schmidt, Advanced Materials **24**, 2668 (2012)

[39] Y. Ma, P. E. Kremer, and B. D. Gerardot, J. of Appl. Phys. **115**, 023106 (2014)

[40] M. Gschrey, M. Seifried, L. Krüuger, R. Schmidt, J.-H. Schulze, T. Heindel, S. Burger, S. Rodt, F. Schmidt, A. Strittmatter, S. Reitzenstein, arXiv:1312.6298 (2013)

[41] W. L. Barnes, G. Björk, J. M. Gérard, P. Jonsson, J. A.E. Wasey, P. T. Worthing, and V. Zwiller, Eur. Phys. J. D **18**, 197 (2002)

[42] R. Trotta, E. Zallo, E. Magerl, O. G. Schmidt, and A. Rastelli, Phyisical Review B **88**, 155312 (2013)